UC Irvine
UC Irvine Previously Published Works

Title
Beam-driven chirping instability in DIII-D (vol 37, pg 937, 1995)

Permalink
https://escholarship.org/uc/item/06v2v3kc

Journal
PLASMA PHYSICS AND CONTROLLED FUSION, 37(11)

ISSN
0741-3335

Author
Heidbrink, WW

Publication Date
1995

Copyright Information
This work is made available under the terms of a Creative Commons Attribution License, availalbe at https://creativecommons.org/licenses/by/4.0/

Peer reviewed

eScholarship.org Powered by the California Digital Library
University of California

Plasma Phys. Control. Fusion 37 (1995) 937–949. Printed in the UK

Beam-driven chirping instability in DIII–D

W W Heidbrink
Department of Physics, University of California, Irvine, CA 92717, USA

Received 22 February 1995, in final form 15 May 1995

Abstract. During neutral-beam injection into the DIII–D tokamak, instabilities with frequencies that 'whistle' down a factor of two in a single 2 ms burst are observed between 50 and 200 kHz. The instabilities have toroidal mode numbers $n = 1$–8 and cause the loss of beam ions from the plasma. In contrast to the usual Alfvén modes, which are fluid modes of the background plasma, these instabilities seem to be beam modes that are nearly stationary in the plasma frame.

1. Introduction

'Fast' ions with speeds considerably greater than thermal speeds are common in tokamak plasmas [1]. Substantial fast-ion populations are produced by neutral-beam injection, by radiofrequency heating, and by fusion reactions. Large fast-ion populations sometimes destabilize instabilities that cause anomalous transport of the fast ions. Anomalous losses degrade the plasma performance and can damage internal vacuum-vessel hardware, so it is important to understand and control fast-ion driven instabilities.

The usual theoretical framework for understanding fast-ion driven instabilities assumes that the fast-ion population is a minor perturbation to the background plasma. If a weakly damped normal mode of the background plasma interacts resonantly with the fast ions, the fast ions can give energy to the wave and drive the wave unstable. Thus, the real part of the frequency ω_r is essentially the frequency of the normal mode, while the fast ions only affect the imaginary part of the frequency γ. For electrostatic modes, this picture is valid if the fast-ion density n_f is much smaller than the density of the background plasma n_e (a condition that is almost always satisfied in practice). For the fast-ion population to have a negligible effect on electromagnetic modes, the fast-ion beta must be small relative to the total beta ($\beta_f/\beta \ll 1$). This condition is sometimes violated in low-density tokamaks with strong auxiliary heating.

When $\beta_f \sim \beta$, new modes are possible [2]. For example, for the fishbone instability, there is a fluid branch with frequency near the diamagnetic frequency ω_{*i} that is a normal mode of the background plasma [3]. The fast-ion mode occurs on a branch with frequencies characteristic of the precessional motion of the fast ions ω_{pre} [4]. Both branches have the $n = 1$ mode structure characteristic of the internal kink. Both branches seem to occur experimentally [1]. Usually, the instabilities occur in bursts of ~ 1 ms duration. In some cases (particularly when $\omega \sim \omega_{*i}$), the mode frequency changes $\lesssim 20\%$ during a burst [5], suggesting identification as a fluid mode. In other cases [6, 7], the frequency is comparable to ω_{pre} and the mode frequency drops a factor of two during a burst, suggesting identification as a fast-ion mode. For example, in PDX [6], the frequency 'whistled' down from 25 to 10 kHz during a fishbone burst.

0741-3335/95/090937+13$19.50 © 1995 IOP Publishing Ltd

Alfvén waves can be driven unstable by a fast-ion population. In a tokamak, the most unstable Alfvén waves are eigenmodes with frequencies in 'forbidden' gaps of the Alfvén continuum. The gaps are created by geometrical effects such as toroidal curvature (the toroidicity-induced Alfvén eigenmode or TAE [8]) or geodesic curvature and plasma compressibility (the beta-induced Alfvén eigenmode or BAE [9]). TAE modes are observed on many tokamaks with several types of fast-ion populations [10–14]. BAE modes are observed during neutral-beam injection into DIII–D [15]. In all cases, the mode frequency is governed by plasma properties such as the Alfvén speed v_A or q profile [16] and scarcely changes on a millisecond timescale, as expected for fluid modes.

Possible hints of a fast-ion branch in the Alfvén range of frequencies were observed on PDX [17] and TFTR [18]. On PDX, bursts with higher frequencies than the fishbone modes 'whistled' down in frequency from 90 to 65 kHz [17], although $\sim$ 80 kHz bursts with constant frequency were also observed [19]. On TFTR, reflectometer diagnostics observe modes that 'chirp' up and down in frequency (as well as the usual TAE modes) [18].

In this paper, we report new observations of instabilities with rapidly changing ('chirping') frequencies in the range of 50–200 kHz. More information on the mode structure is given than in previous studies. In addition, the relationship between the chirping modes and the fluid Alfvén modes is clarified. It is found that chirping occurs when the fast-ion beta β_f, the Alfvén speed v_A, and the plasma rotation are all relatively large.

2. Experiment

Chirping instabilities are rarely observed on the magnetic probes in DIII–D: of $\sim$ 1000 discharges examined for evidence of Alfvén activity, only six discharges have chirping modes. All six discharges are from the same day of low density, high-power operation. These discharges are double-null divertor deuterium plasmas (figure 1). To obtain clean, low-density plasmas (typically $\bar{n}_e = 2.5 \times 10^{13}$ cm^{-3} and $Z_{eff} \simeq 1.5$), the boron-coated walls are baked to $\sim 300\,^{\circ}$C the day before the experiment and glow discharge cleaning is employed after each discharge. Near tangential (tangency radius $R_{tan} \simeq 1.10$ m), $\sim$ 75 keV deuterium neutrals are injected in the direction of the plasma current. The plasma current is $I_p = 0.6$ MA and the toroidal field is varied between $B_T = 1.0$ and 1.7 T.

The plasma shape and q profile are obtained from the magnetic configuration and eight central motional Stark effect (MSE) polarimetry measurements [20] using the fitting code EFIT [21]. Electron temperature and density profiles are measured by Thomson scattering [22]. Ion temperature and toroidal rotation speed profiles are obtained from charge exchange recombination spectroscopy, utilizing one of the heating beams [23]. The neutron flux is measured with plastic and ZnS scintillators [24] that are cross-calibrated to a set of absolutely calibrated neutron counters [25]. Fluctuation diagnostics include extensive poloidal and toroidal arrays of magnetic probes mounted inside the vacuum vessel (figure 1). Toroidal mode numbers n are obtained from the best fit to the phase differences of a toroidal array of eight probes. Radial information about the fluctuations is obtained from an array of soft x-ray detectors (figure 1), reflectometer channels [26], and a far-infrared laser scattering diagnostic [27].

Figure 2 shows a large $n = 3$ chirping mode. The mode frequency decreases from $\sim$ 100 to $\sim$ 55 kHz during the $\sim$ 2.5 ms burst. The burst correlates with a reduction in neutron emission, indicating transport of beam ions by the mode (see below). Both the mode frequency and the neutron flux decrease rapidly when the mode amplitude is large.

Like other beam-driven instabilities [1], the modes with chirping frequencies occur in bursts. Several bursts are shown in figure 3 (the burst shown in figure 2 is the elongated

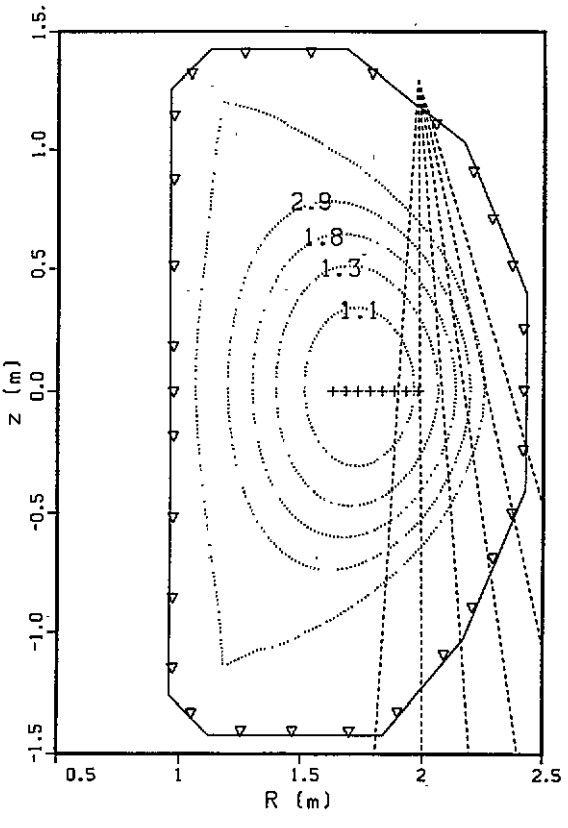

Figure 1. Elevation of DIII–D. The dotted curves indicate the plasma configuration inferred from a fit to magnetics data and eight MSE measurements (+); the values of q for the discharge shown in figure 5 are given. The broken curves are the soft x-ray sightlines for the data shown in figure 5. The locations of the poloidal array of Mirnov coils (figure 6) are also indicated (▽).

vertical 'sausage' at 1663 ms in this contour plot). Figure 3 is typical: the burst cycle is highly variable both in amplitude and period. Even the mode number of the chirping mode differs on successive bursts. Generally, there are two types of chirping modes. One is a 'pure' mode with a single toroidal mode number, such as the burst shown in figure 2. There are also 'multiple' chirping modes, such as the burst shown at 1679 ms in figure 3. In a multiple chirping mode, the $n = 1$ amplitude is initially dominant (figure 4). As the burst evolves, the magnetic waveform becomes increasingly distorted (from a sinusoidal shape) and higher harmonics appear in the spectrum. Then, as the burst begins to decay, something unusual happens. The $n = 1$ mode decays more rapidly in amplitude than its 'harmonics' so that, at the end of the burst, only the higher mode numbers remain (cf the $n = 4$ mode at 1685 ms in figures 3 and 4). In the example of figure 4, the ratio of $n = 4$ amplitude to $n = 1$ amplitude is only $\tilde{B}_4/\tilde{B}_1 = 0.02$ at the peak of the instability, but $\tilde{B}_4/\tilde{B}_1 = 4$ at the time of maximum amplitude of the $n = 4$ mode. Apparently an initially unstable $n = 1$ mode excites an $n = 4$ mode, which then decays more slowly than the 'fundamental' instability. Another example of a multiple mode appears in figure 5.

For both pure and multiple chirping modes the frequency drops a factor of two during a burst. The observed mode frequency is affected by the Doppler shift [28]. Approximately, the frequency in the laboratory frame f_{lab} is related to the frequency in the plasma frame

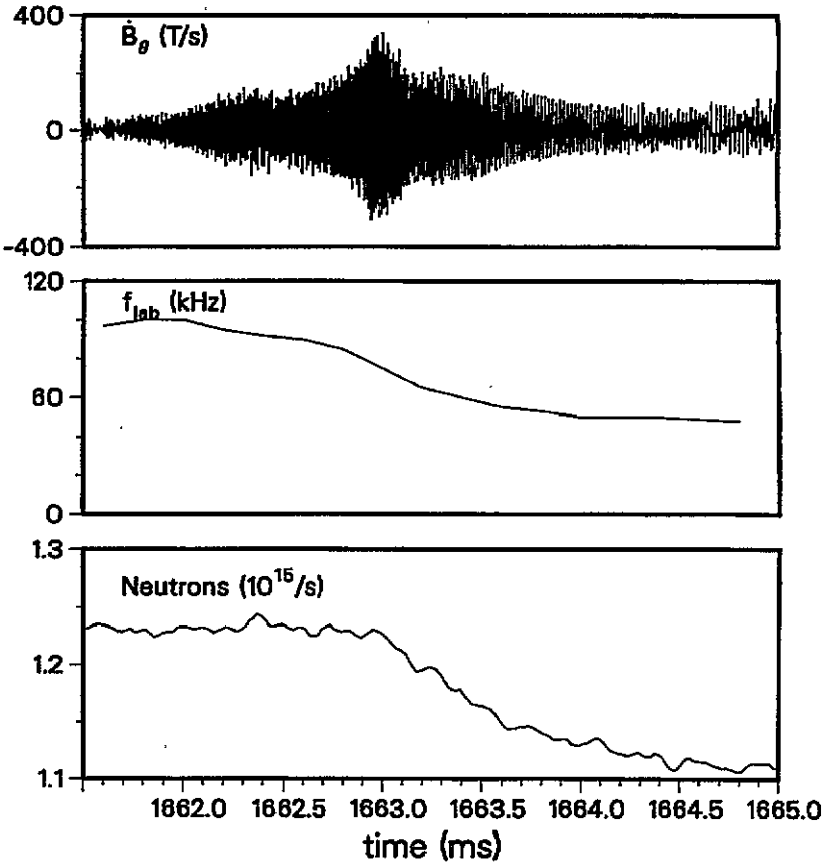

Figure 2. Magnetic probe signal, frequency of the magnetic oscillation, and neutron emission during a 'chirping' burst. $B_T = 1.7$ T; $I_p = 0.62$ MA; $\bar{n}_e = 2.5 \times 10^{13}$ cm^{-3}; $P_B = 12.2$ MW; $T_e(0) = 3.1$ keV; $T_i(0) \simeq 12$ keV.

f_{pl} and the toroidal rotation frequency f_{rot} by

$$F_{lab} \simeq f_{pl} + nf_{rot} \tag{1}$$

where n is the toroidal mode number. Because of the large angular momentum of the background plasma, it is unlikely that the plasma rotation profile $f_{rot}(r)$ changes appreciably during a burst. The rotation profile is sheared, however, so $f_{rot}(r)$ decreases with increasing minor radius. Thus, the frequency could drop for one of two reasons: f_{pl} may decrease or the mode may shift to larger radius where the Doppler shift nf_{rot} is smaller.

The available measurements of the spatial structure are somewhat inconclusive, but suggest little shift to larger radii. In a pure chirping mode, the toroidal mode number remains constant throughout a burst. Reflectometer channels detect the instability in the scrapeoff plasma (possibly due to fast ions that are expelled from the plasma). The far-infrared laser scattering diagnostic also detects the chirping instability, but the spatial resolution is too coarse to detect a shift in spatial structure. The fluctuations measured by six soft x-ray channels during a multiple chirping mode are shown in figure 5. Because the soft x-ray measurement is a chordal measurement, edge fluctuations may contribute to all of the signals. Nevertheless, it is apparent that the instability has a substantial amplitude in the

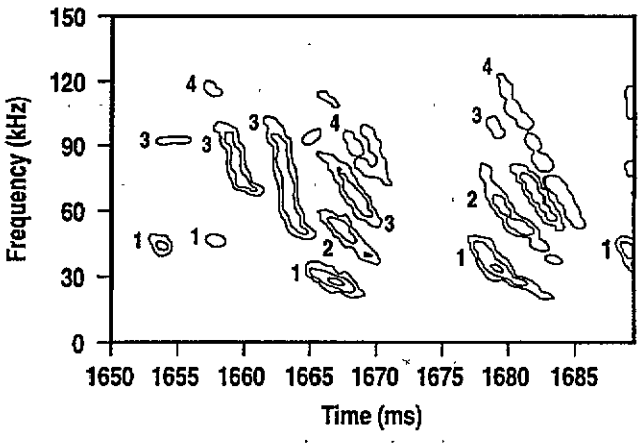

Figure 3. Logarithmic contours of the amplitude of a magnetic probe signal for the same discharge as in figure 2. The toroidal mode numbers are indicated. Pure chirping modes occur at 1659 and 1663 ms; multiple chirping modes occur at 1667 ms and 1679 ms.

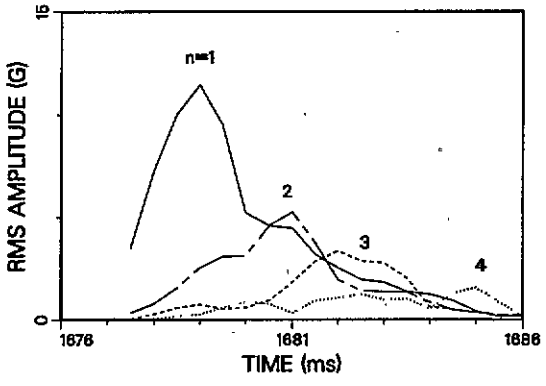

Figure 4. Amplitudes of the first four toroidal modes for the multiple chirping mode shown in figure 3.

interior of the plasma. There may be some shift outward in radius as the burst evolves, but the evolution of the various signals is fairly similar.

The poloidal array of magnetic probes (figure 1) suggests the spatial structure barely changes during a burst. Figure 6 shows the data at three times during the multiple burst of figure 5. No significant alteration in structure is detected. However, since the probe signals are most sensitive to fluctuations at the plasma edge, these data do not exclude the possibility of internal rearrangement. Similar probe results are obtained for pure chirping modes.

The chirping modes appear to satisfy two separate conditions simultaneously: the laboratory frequency $f_{\rm lab}$ is comparable to the circulation frequency of the beam ions $f_{\rm circ} = v_{\|}/q2\pi R$; *and* the frequency in the plasma frame $f_{\rm pl}$ is nearly zero. To study the chirping modes, a database of 21 pure chirping modes, three multiple chirping modes, and six BAE modes was assembled. A representative sample of chirping modes from all six discharges that exhibit the instability was selected. One discharge on this day (shot 81410) had parameters similar to the discharges with chirping modes, but exhibited BAE activity instead. This discharge and the five discharges in the toroidal field scan of [15] were selected as representative of plasmas with BAE activity. (A detailed study of BAE modes in DIII–D is the topic of a future paper.) In addition, a representative sample of 43 fishbone

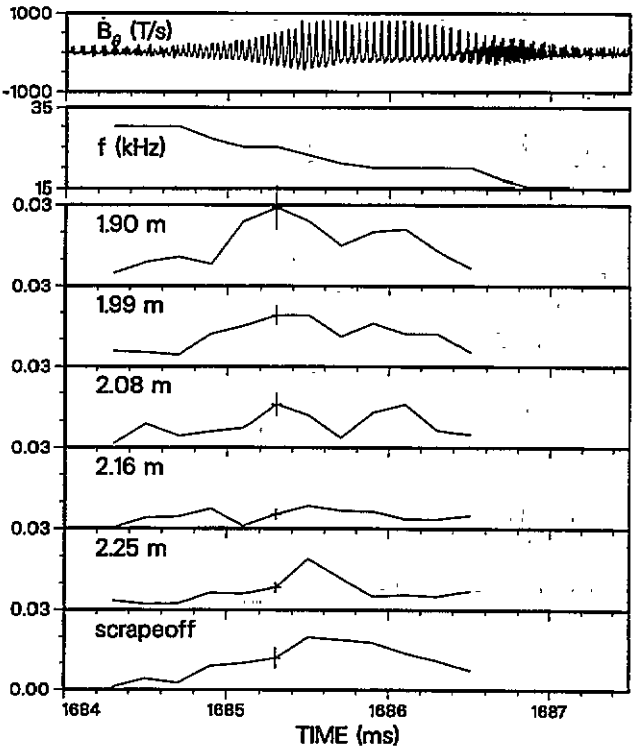

Figure 5. Magnetic probe signal, frequency of the magnetic oscillation, and soft x-ray fluctuation amplitudes $\tilde{S}$ during a multiple chirping burst. The fluctuation amplitude is measured at the frequency of the $n = 1$ chirping mode (determined from the magnetics signal), which evolves in time. The labels are the equivalent radii (at the outer midplane) of the innermost flux surface viewed by each channel; the actual chords and flux-surface geometry are shown in figure 1. The DC levels S for the six channels are 0.22, 0.17, 0.13, 0.10, 0.07, and 0.03, respectively. Typical errors (crosses) are estimated by analysing the amplitude 5 kHz from the peak. $B_T = 1.0$ T; $I_p = 0.62$ MA; $\bar{n}_e = 2.5 \times 10^{13}$ cm^{-3}; $P_B = 9.5$ MW; $T_e(0) = 2.3$ keV; $T_i(0) \simeq 7$ keV; central toroidal rotation frequency $f_{rot}(0) \simeq 30$ kHz.

instabilities was obtained from the discharges described in [29].

In contrast to BAE modes, the modes with chirping frequencies tend to be stationary in the plasma frame (figure 7). The ratio $f_{lab}/f_{rot}(0)$ scales linearly with n (figure 7(a)), suggesting that the laboratory frequency is determined primarily by the Doppler shift ($f_{lab} - nf_{rot} = f_{pl} \simeq 0$). Indeed, the ratio $f_{lab}/(nf_{rot}(0)) \simeq 0.8$ is nearly constant (figure 7(b)), as expected for a mode that is stationary near the centre of the plasma. Both the frequency at maximum amplitude f_{lab}^{max} (figure 7) and the frequency at the beginning of the burst f_{lab}^{beg} scale linearly with $nf_{rot}(0)$. In all cases, the laboratory frequency is comparable to the beam circulation frequency f_{circ}, but the dependence is weak and, after taking into account the Doppler shift, there is no dependence of $f_{lab}/(nf_{rot}(0))$ on B_T, q_0, or q_{95} (the q at the flux surface that encloses 95% of the flux). Pure chirping modes with $n = 3$–8 are observed.

The chirping frequencies fall below the Alfvén continuum of ideal MHD (figure 8), in the same gap where BAE modes are observed [15]. Although the frequencies in the laboratory frame are comparable to BAE modes, the frequency in the plasma frame is lower,

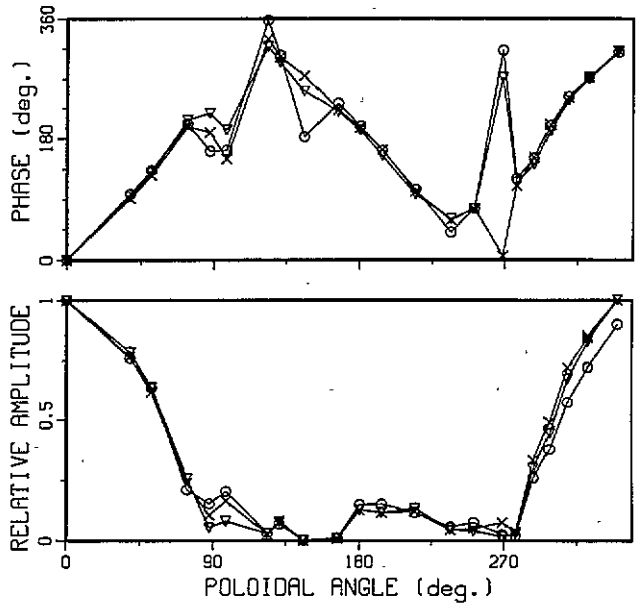

Figure 6. Phase angle and amplitude of the magnetic fluctuations as a function of poloidal angle for the $n = 1$ component of the multiple chirping burst shown in figure 5. (○) 1684.4 ms; (▽) 1685.2 ms; (×) 1686.3 ms. The angle is measured relative to the outer midplane (0°).

because the chirping modes occur in plasmas that are rotating rapidly (compare figure 4 of [15] with figure 8). The initial laboratory frequency is comparable to the circulation frequency of the beam ions $f_{\rm circ} = v_\parallel/q2\pi R$ in the plasma centre. Interestingly, $f_{\rm lab} = f_{\rm circ}$ at approximately the same radius that $f_{\rm pl} \simeq 0$. As the burst evolves, $f_{\rm lab}$ decreases, so the radius where $f_{\rm lab} = f_{\rm circ}$ increases, but the rotation profile is such that $f_{\rm pl} \simeq 0$ at this position too (figure 8). In contrast, for BAE modes, $f_{\rm pl} > 0$ everywhere in the plasma.

Apparently, three conditions are required for chirping instability. First, the rotation frequency must be sufficiently large that the conditions $f_{\rm pl} \simeq 0$ and $f_{\rm lab} \sim f_{\rm circ}$ are simultaneously satisfied. The most obvious difference in plasma parameters between plasmas with chirping modes and those with BAE activity is that $f_{\rm rot}(0)$ is larger in discharges with chirping activity (figure 7(*b*)). A second requirement is a large beam-ion population ($\langle\beta_{\rm f}\rangle \gtrsim 1\%$), a condition that is also required for Alfvén activity (figure 9). A possible third condition is a low value of $v_\parallel/v_{\rm A}$. Theoretically, the fast-ion drive for TAE modes is an order of magnitude larger for $v_\parallel \geqslant v_{\rm A}$ than for $v_{\rm A}/3 < v_\parallel < v_{\rm A}$ [31]. Finite-orbit width effects broaden this sharp resonance [32]. Empirically, in DIII–D plasmas with $I_{\rm p} \simeq 0.6$ MA, the transition from the fundamental drive ($v_\parallel = v_{\rm A}$) to the sideband drive ($v_\parallel = v_{\rm A}/3$) occurs when $v_{\parallel 0}/v_{\rm A} \simeq 0.6$ [33]. All of the observed chirping modes occur at low values of $v_\parallel/v_{\rm A}$ (figure 9), where only the sideband drive is operative for the fluid Alfvén modes.

The chirping modes transport beam ions to the edge of the plasma. Bursts of magnetic activity correlate with drops in neutron emission (figure 10). In plasmas with appreciable beam–plasma reactions, reductions in neutron emission indicate the loss of beam ions from the plasma centre [17, 34]. During the 1992 and 1993 campaigns, the outer wall of the DIII–D vessel was axisymmetric and foil-bolometer measurements of the heat flux could be used to infer the amount of beam-ion energy lost to the walls [34]. For the 1994 campaign,

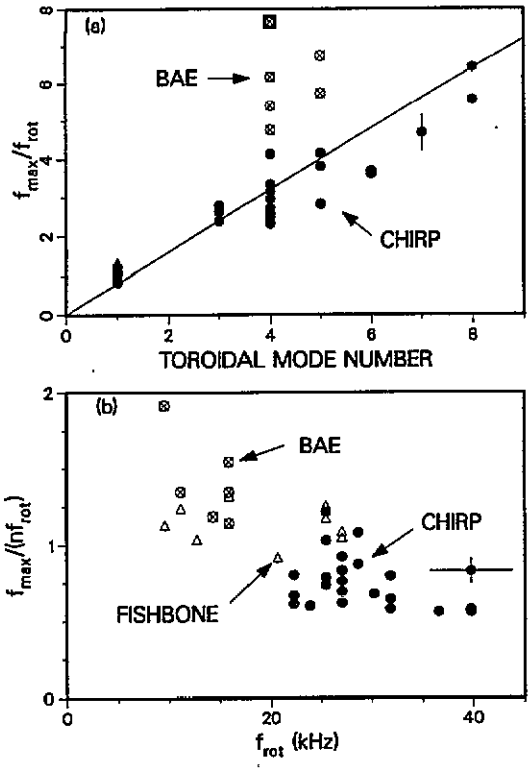

Figure 7. (*a*) Ratio of the frequency at peak mode amplitude f_{max} to the central plasma rotation frequency $f_{rot}(0)$ as a function of the toroidal mode number n for chirping modes (●), BAE modes (⊠), and $n = 1$ fishbone modes (△). The line shows the expected dependence for stationary modes ($f_{pl} = 0$) that rotate at 80% of the central rotation speed. (*b*) Ratio of f_{max} to the central Doppler shift $nf_{rot}(0)$ as a function of the central rotation frequency. The error bars represent an estimate of the uncertainty in $f_{rot}(0)$ (the dominant uncertainty).

new ICRF (ion cyclotron range of frequencies) antennae that project past the outer wall were added to the machine. In the modified vessel, escaping beam ions bombard the Faraday shields and protective limiters of the ICRF antenna. In the presence of beam-ion losses, both the Faraday shields and the (recessed) foil bolometers glow when viewed with an infrared camera. The bombardment also causes increased stray light in the vicinity of the Faraday shield. The shield is in the field of view of the edge channels of the 16-channel MSE diagnostic [20], and the stray light causes a prompt reduction in the polarimetry signal, as shown in figure 10. (The stray light may be caused by a bright carbon line in the wings of the 6600 ± 3 Å filter or by enhanced bremsstrahlung.) Within the accuracy of the measurement, the reductions in MSE signal are synchronous with the reductions in neutron flux. The magnitude of the reductions also correlate well (correlation coefficient $r^2 = 0.88$). The neutron, infrared camera, and MSE observations confirm that chirping modes cause the loss of some beam ions from the plasma.

For pure chirping modes, the magnitude of the losses scales roughly linearly with the mode amplitude (figure 11). No significant dependence on toroidal mode number n or toroidal field (or q) is observed. The correlation with $\dot{B}$ is similar to the correlation with $\tilde{B}$. For a given amplitude at the edge, the chirping modes cause much smaller losses of beam ions than BAE or TAE modes but much larger losses than fishbone modes (figure 11).

Within a burst, the loss rate is greatest when the mode amplitude is largest. For the bursts in our database, the maximum gradient in the neutron emission $-\mathrm{d}I_n/\mathrm{d}t$ lags the peak amplitude of the burst $\dot{B}_{max}$ by 0.07 ± 0.20 ms. Similar behaviour was observed for fishbone bursts [17] and TAE bursts [34]. Concurrently, the mode frequency drops most rapidly when the mode amplitude peaks. (The maximum value of $-\mathrm{d}f_{lab}/\mathrm{d}t$ leads $\dot{B}_{max}$ by 0.14 ± 0.15 ms.) This is also similar to the temporal evolution of a fishbone burst [7, 17, 19].

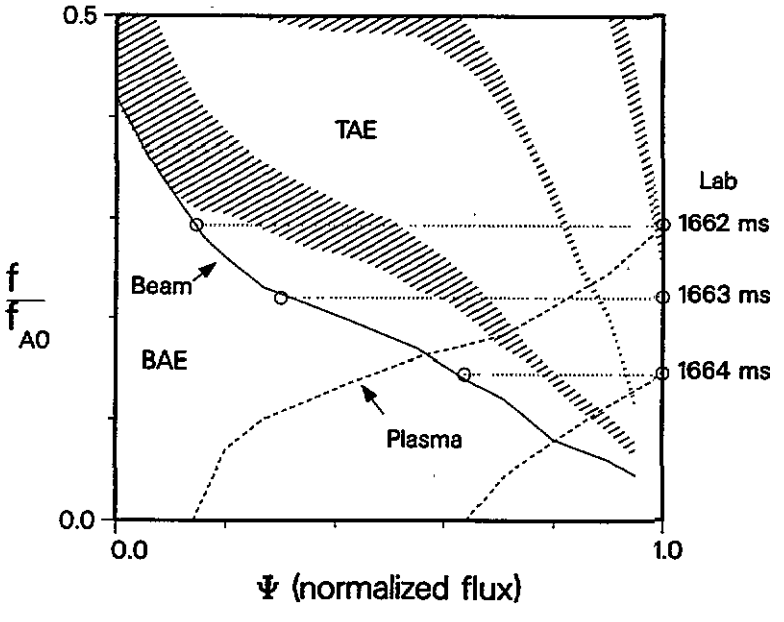

Figure 8. Doppler-shifted frequency in the plasma $f_{\rm pl}$ (dotted curves) against normalized poloidal flux for the burst shown in figure 2. The frequency in the plasma frame is obtained from the measured frequency $f_{\rm lab}$ (circles) and the measured toroidal rotation frequency $f_{\rm rot}(\Psi)$ using equation (1). The shaded regions are the Alfvén continuum of ideal MHD calculated by the CONT code [30]; the chirping mode lies in the BAE gap. The full curve is the expected frequency $v_{\|0}/2\pi qR$ of a beam mode that is resonant with full energy beam ions at the nominal angle of beam injection, $v_{\|0} = v_{\rm b}R_{\rm tan}/R_0$, where $v_{\rm b}$ is the injection speed and R_0 is the radius of the magnetic axis. All of the frequencies are normalized to the Alfvén frequency on axis $f_{\rm A0} = 340$ kHz. The uncertainty in the rotation profile is approximately ±10%, which propagates into a ~ 10% error in the Doppler-shift correction. Uncertainty in the equilibrium reconstruction is estimated to yield variations in the curves of 5–10%.

Table 1. Typical characteristics of DIII–D beam-driven instabilities.

Mode	$f_{\rm lab}$ (kHz)	$\Delta f/f$ (%)	n	$v_{\|0}/v_{\rm A}$	$\langle\beta_{\rm f}\rangle$ (%)	$f_{\rm rot}$ (kHz)	$\tilde{B}_\theta$ (G)	Neutron drop (%)
Chirping	80	40–110	1–8	0.3–0.5	$\gtrsim$1	30	4	10
BAE	80	$\lesssim$3	1–10	0.2–1.0	$\gtrsim$1	12	0.4	15
TAE	110	$\lesssim$2	1–10	0.3–1.0	$\gtrsim$1	12	0.4	15
Fishbone	20	$\lesssim$10	1	0.2–1.0	$\gtrsim$0.3	15	4	$\lesssim$2

The characteristics of the four types of beam-driven instabilities observed in DIII–D are compared in table 1. The distinctive feature of the chirping mode is the large variation in frequency $\Delta f/f$ during a burst. Other distinctive traits are the rarity of occurrence, and the fact that modes with chirping frequencies have only been observed for $v_{\|0}/v_{\rm A} < 0.5$ and $f_{\rm rot} > 20$ kHz.

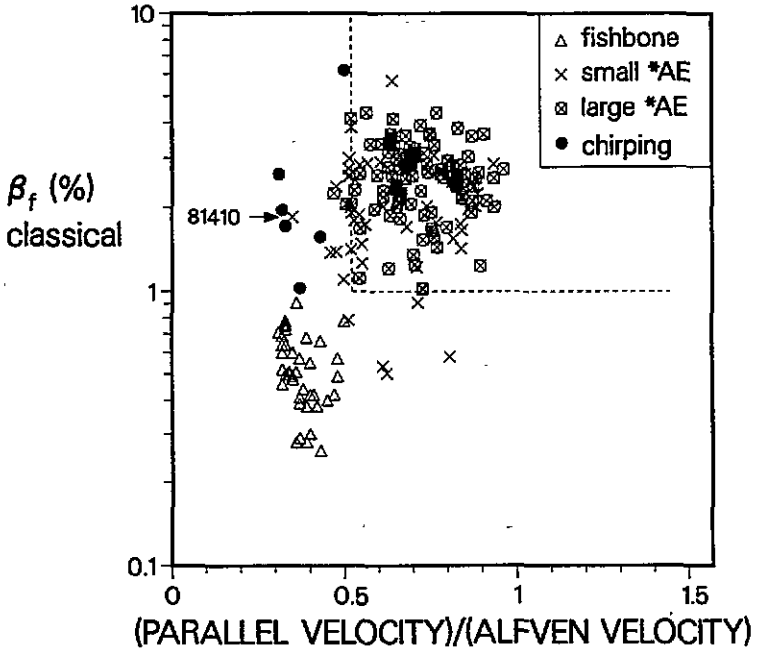

Figure 9. Relationship of the discharges with chirping activity (●) to discharges with TAE and BAE activity (through the 1992 campaign) [33] (× and ⊠) and to discharges with fishbone modes [29] (△). The ordinate represents the classically estimated, volume-averaged beam ion beta ($\langle\beta_{fc}\rangle$). (The actual value may be reduced by fast-ion losses.) The abscissa represents the ratio of the parallel velocity of full-energy beam ions that ionize on axis $v_{\|0}$ to the Alfvén speed v_A (evaluated using B_T and $\bar{n}_e$). The dotted curves demarcate the approximate thresholds in $\langle\beta_{fc}\rangle$ and $v_{\|0}/v_A$ for strong Alfvén activity in DIII–D. The chirping modes and the comparison discharge with BAE activity (81410) were all acquired on the same day in 1994.

3. Discussion

The experimentally observed chirping modes may be related to the energetic-particle continuum mode discussed by Tsai and Chen [35] in their paper about kinetic ballooning modes. Tsai and Chen predict a mode frequency of $0.83v_\|/q2\pi R$, which is comparable to the experimental observations (figure 8). They also predict a threshold condition for instability

$$\alpha_f \gtrsim 0.7 s v_\|/v_A \tag{2}$$

where $\alpha_f = -q^2 R_0 \, d\beta_f/dr$ is proportional to the fast-ion pressure gradient and $s = rq'/q$ is the shear parameter. Because of the relatively large value of β_f ($\alpha_f \sim 0.2$), the relatively low value of $v_\|/v_A$ (~ 0.3), and the modest value of s (~ 0.5) in these shaped DIII–D plasmas, equation (2) is satisfied in the plasma interior for the discharges with chirping modes. Qualitative considerations are also consistent with theory. One expects beam modes to occur at low values of $v_\|/v_A$, where the interaction with Alfvén modes is relatively weak, and this is the experimental observation (figure 9). The modes occur in plasmas where β_f is a significant fraction ($\gtrsim 1/3$) of the total β, as expected for an electromagnetic beam mode.

The theory of [35] neglects plasma rotation, but this is clearly important in the experiment (figure 7). Experimentally, chirping modes seem to select values of n and f_{lab} that cause the conditions $f_{pl} \simeq 0$ and $f_{lab} \sim f_{circ}$ to be satisfied simultaneously. We

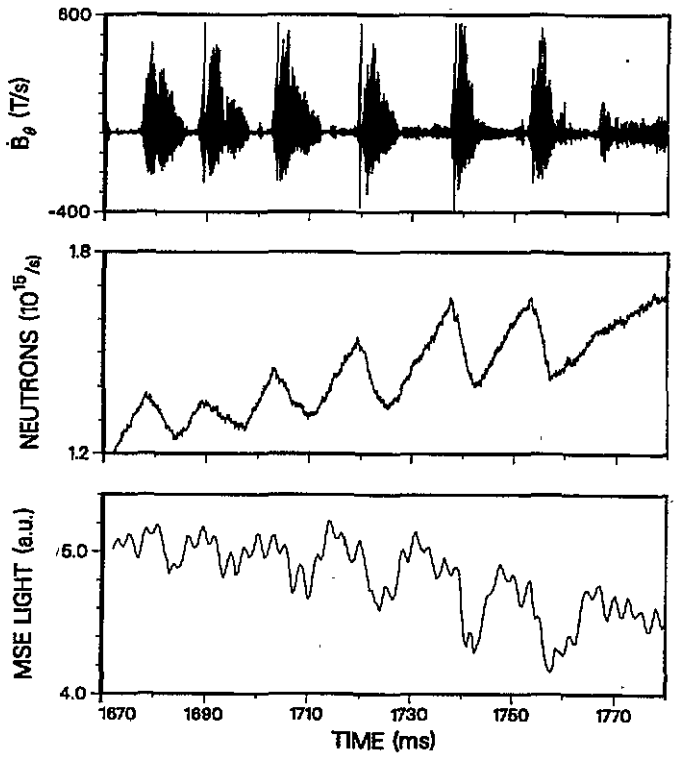

Figure 10. Magnetic probe signal, neutron flux, and MSE background light from two edge channels for the discharge shown in figure 2. The vertical 'spikes' on the magnetic probe signal are ELMs; the longer bursts are chirping modes.

speculate that the first condition minimizes the energy required to excite the mode, while the second condition is necessary to extract energy from the fast-ion population. Presumably, the second condition is less stringent than the first because the fast-ion distribution function spans a wide range in parallel velocity.

It is not clear why the mode frequency drops so dramatically. Figure 8 suggests that the mode 'tracks' a resonant population of fast ions as they move outward radially. (This idea was first proposed to explain the drop in frequency at a fishbone burst [4].) The chirping modes may act as a naturally occurring 'bucket' in phase space that transports beam ions to the plasma edge [36, 37]. Alternatively, the resonant population may lose energy, causing $f_{\rm circ}$ to decrease in time at a fixed spatial location. A third possibility is that, as the mode amplitude grows, magnetic interaction with the vessel or with uncorrected error fields exerts a torque on the mode, causing it to slow down.

The time evolution of the multiple chirping modes is particularly intriguing (figure 4). A possible explanation for the transition from $n = 1$ activity early in the burst to higher n activity later in the burst is that, as the $n = 1$ frequency drops below ~ 20 kHz, it becomes too small to interact effectively with the beam-ion population (i.e. $f_{\rm lab} \simeq n f_{\rm rot}$ becomes smaller than $f_{\rm circ}$ for $n = 1$). At this frequency, the $n = 3$ or $n = 4$ 'harmonics' (at 60 or 80 kHz) resonate more strongly with the fast ions, so the higher harmonics persist after the $n = 1$ mode has decayed away.

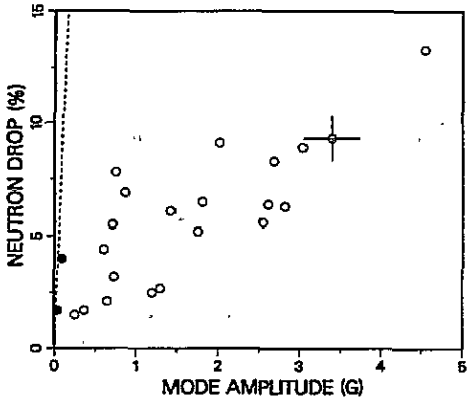

Figure 11. Fractional reduction in neutron emission against the amplitude of the burst $\tilde{B}_\theta$ for pure chirping modes (●) and for fishbone modes (△). The data are drawn from the six discharges with chirping modes (n = 3–8, B_T = 1.0–1.7 T). The dotted curve is the scaling observed for TAE and BAE modes in DIII–D [34] and the ⊠ symbols represent values observed for BAE modes in the comparison discharge 81410. (The amplitude $\tilde{B}_\theta$ is approximated by $\dot{B}_{RMS}/2\pi F_{lab}^{max}$, where $\dot{B}_{RMS}$ is defined in [34].) The error bar represents the typical random error associated with the analysis techniques.

For a given mode amplitude, the chirping modes are much less effective in transporting beam ions than Alfvén instabilities (figure 11), possibly suggesting a weaker resonant interaction. This may explain why Alfvén modes are normally observed in plasmas with large values of β_f, while chirping modes are a rarity.

4. Conclusion

Modes with frequencies that drop a factor of two during a burst are observed in the DIII–D tokamak. Many toroidal mode numbers occur (n = 1–8). The modes are nearly stationary in the plasma frame, but have frequencies that allow for resonant interaction with the circulating beam ions. The instabilities cause fast-ion loss. The modes are rare compared to the fluid Alfvén modes, apparently requiring a combination of large plasma rotation, large fast-ion beta, and low ratio of beam speed to Alfvén speed. The chirping modes seem to represent a 'beam' branch that lies in the frequency gap below the Alfvén continuum. A complete theoretical treatment of these modes will include the effects of plasma rotation.

Acknowledgments

The many contributions of the DIII–D team are gratefully acknowledged. Assistance with the analysis was provided by Reed James (figures 1 and 8), Ted Strait (figures 1, 3 and 4), Brad Rice (figure 10), Rich Groebner (figure 7), Jinchoon Kim (figure 8), and Transon Nguyen (figures 7 and 11). Helpful suggestions by Edward Doyle, Liu Chen, Mike Mauel, and Bob Santoro are also appreciated. This work was supported by Subcontract SC-L134501 of US Department of Energy Contract DE-AC03-89ER51114.

References

[1] Heidbrink W W and Sadler G J 1994 *Nucl. Fusion* **34** 535

[2] Chen L 1994 *Phys. Plasma* **1** 1519
[3] Coppi B and Porcelli F 1986 *Phys. Rev. Lett.* **57** 2272
[4] Chen L, White R B and Rosenbluth M N 1984 *Phys. Rev. Lett.* **52** 1122
[5] Heidbrink W W and Sager G 1990 *Nucl. Fusion* **30** 1015
[6] McGuire K *et al* 1983 *Phys. Rev. Lett.* **50** 891
[7] Nave M F F *et al* 1991 *Nucl. Fusion* **31** 697
[8] Cheng C Z and Chance M S 1986 *Phys. Fluids* **29** 3695
[9] Turnbull A D *et al* 1993 *Phys. Fluids* B **5** 2546
[10] Wong K L *et al* 1991 *Phys. Rev. Lett.* **66** 1874
[11] Heidbrink W W, Strait E J, Doyle E, Sager G and Snider R T 1991 *Nucl. Fusion* **31** 1635
[12] Wong K L *et al* 1994 *Plasma Phys. Control. Fusion* **36** 879
[13] Ali-Arshad S and Campbell D J 1995 *Plasma Phys. Control. Fusion* **37** 715
[14] Mori M and JT-60 team 1994 *Plasma Phys. Control. Fusion* **36** B181
[15] Heidbrink W W, Strait E J, Chu M S and Turnbull M S 1993 *Phys. Rev. Lett.* **71** 855
[16] Heidbrink W W 1994 *Theory of Fusion Plasmas (Proc. Joint Varenna–Lausanne Workshop 1994)* (Bologna: Editrice Compositori) p 49
[17] Strachan J D *et al* 1985 *Nucl. Fusion* **25** 863
[18] Mazzucato E *et al* 1992 *Proc. 19th EPS (Innsbruck, 1992)* vol 16C (Petit-Lancey: EPS) p 1055
[19] Buchenauer D A J 1985 Fast ion effects on magnetic instabilities in the PDX tokamak *PhD Thesis* Princeton University
[20] Rice B W, Nilson D G and Wroblewski D 1995 *Rev. Sci. Instrum.* **66** 373
[21] Lao L L, St John H, Stambaugh R D, Kellman A G and Pfeiffer W P 1985 *Nucl. Fusion* **25** 1611
[22] Carlstrom T N *et al* 1992 *Rev. Sci. Instrum.* **63** 4901
[23] Gohil P, Burrell K H, Groebner R J and Seraydarian R P 1990 *Rev. Sci. Instrum.* **61** 2949
[24] Heidbrink W W 1986 *Rev. Sci. Instrum.* **57** 1769
[25] Strachan J D *et al* 1990 *Rev. Sci. Instrum.* **61** 3501
[26] Lehecka T *et al* 1988 *Rev. Sci. Instrum.* **59** 1620
[27] Philipona R *et al* 1990 *Rev. Sci. Instrum.* **61** 3007
[28] Strait E J, Heidbrink W W and Turnbull A D 1994 *Plasma Phys. Control. Fusion* **36** 1211
[29] Heidbrink W W and Danielson J R 1994 *Phys. Plasma* **1** 4120
[30] Chu M S, Greene J M, Lao L L, Turnbull A D and Chance M S 1992 *Phys. Fluids* B **4** 3713
[31] Betti R and Freiberg J P 1992 *Phys. Fluids* B **4** 1465
[32] Fu G Y and Cheng C Z 1992 *Phys. Fluids* B **4** 3722
[33] Strait E J, Heidbrink W W, Turnbull A D, Chu M S and Duong H H 1993 *Nucl. Fusion* **33** 1849
[34] Duong H H *et al* 1993 *Nucl. Fusion* **33** 749
[35] Tsai S-T and Chen L 1993 *Phys. Fluids* B **5** 3284
[36] Hsu C T, Cheng C Z, Helander P, Sigmar D J and White R 1994 *Phys. Rev. Lett.* **72** 2503
[37] Mynick H E and Pomphrey N 1994 *Nucl. Fusion* **34** 1277